

Shapley-PC: Constraint-based Causal Structure Learning with Shapley Values

Fabrizio Russo¹ and Francesca Toni¹

¹Imperial College London
{fabrizio,ft}@imperial.ac.uk

Abstract

Causal Structure Learning (CSL), amounting to extracting causal relations among the variables in a dataset, is widely perceived as an important step towards robust and transparent models. Constraint-based CSL leverages conditional independence tests to perform causal discovery. We propose *Shapley-PC*, a novel method to improve constraint-based CSL algorithms by using Shapley values over the possible conditioning sets to decide which variables are responsible for the observed conditional (in)dependencies. We prove soundness and asymptotic consistency and demonstrate that it can outperform state-of-the-art constraint-based, search-based and functional causal model-based methods, according to standard metrics in CSL.

1 Introduction

Causal Structure Learning (CSL), also referred to as Causal Discovery, is the process of extracting the causal relationships among variables in data, and represent them as graphs. Learning (causal) graphs is important because of their causal interpretation. It corresponds to collecting and validating, with data, the assumptions necessary to perform causal inference, e.g. with causal graphical models [Peters et al., 2017] or Functional Causal Models (FCM) [Spirtes et al., 2000; Pearl, 2009], for the estimation of causal effects, such as the impact of an action or treatment on an outcome. Causal effects are ideally discovered through interventions or randomised control trials, but these can be expensive, time consuming or unethical, e.g. establishing if smoking causes cancer. Hence the need to use observational, as opposed to interventional, data to study causes and effects [Peters et al., 2017; Schölkopf et al., 2021].

CSL has been studied extensively in various settings and a number of methods have been proposed to address the challenge (see e.g. [Glymour et al., 2019; Vowels et al., 2022; Zanga et al., 2022] for overviews). The literature is broadly divided into three classes of methods:

constraint-based, score-based and FCM-based methods (for details see Section 2). In this paper, we provide a novel constraint-based method.

Constraint-based methods use conditional independence tests and graphical rules based on d-separation [Pearl, 2009] to recover as much of the causal structure as possible, under different assumptions [Colombo and Maathuis, 2014]. Under the assumption of causal sufficiency, i.e. that no latent common causes are missing from the data, the Peter Clark (PC)-algorithm [Spirtes et al., 2000] recovers a graph encoding as much of the discoverable relations as possible (see Section 3). Depending on the assumptions, the output of constraint-based methods may be sound and complete [Spirtes et al., 2000] and asymptotically consistent [Kalisch and Bühlman, 2007; Harris and Drton, 2013]. However, with a finite sample, errors can emerge from the multiple conditional independence tests performed.

In this paper we propose a novel method addressing the finite sample performance of PC, by analysing the results of conditional independence tests using an established game-theoretical concept, Shapley values [Shapley, 1953]. Generally, Shapley values are a quantification of the contribution of an entity to an output created by a group of entities. They have been used in settings ranging from economics [Ichiishi, 1983] to machine learning [Lundberg and Lee, 2017; Frye et al., 2020; Heskes et al., 2020] because of their properties, but, to the best of our knowledge, they have not been used for CSL. Overall, our contributions in this paper are:

- We propose a novel decision rule that can be applied to constraint-based CSL algorithms to guide the search for v-structures. We implement our method within the PC-stable algorithm [Colombo and Maathuis, 2014], obtaining the *Shapley-PC* algorithm and prove that the soundness and consistency of the original PC-algorithm are preserved with infinite data (Section 4).
- We provide an extensive evaluation of Shapley-PC compared to several constraint-based, score-based and FCM-based baselines. Our experiments provide empirical evidence about the value-added of our decision rule, consistently outperforming PC-

based predecessors using the same information extracted from data. Furthermore, we analyse the graph characteristics and the data generating processes that best fit the different methods compared, and show how our proposed algorithm performs consistently across a wide range of scenarios (Section 5).

2 Related Work

As mentioned in the introduction, the literature on CSL is broadly divided into three main approaches: constraint-based, score-based and functional causal model (FCM)-based methods. For a comprehensive overview we refer the reader to [Glymour et al., 2019; Vowels et al., 2022; Zanga et al., 2022].

Constraint-based CSL algorithms are based on conditional independence tests and graphical rules based on the d-separation criterion [Pearl, 2009]. They usually assume faithfulness, under which they can be proved sound and asymptotically consistent. The PC-Algorithm [Spirtes et al., 2000] is considered the first efficient method to carry out the task, and many modifications have been proposed to improve different aspects of it. We describe the methods most closely related to ours in detail in Section 3.4, since they help contextualise our proposal, which falls in this category. Lifting the sufficiency assumption, fast causal inference [Spirtes et al., 2000; Colombo et al., 2012]) output partial ancestral graphs, capturing the effect of latent confounders. Lifting the acyclicity assumption, the CCD-algorithm [Richardson and Spirtes, 1999] provably recovers a (partially) directed but not necessarily acyclic graph. Also fast causal inference has been shown to work in cyclic settings [Mooij and Claassen, 2020]. Finally, Ng et al. [2021] relax the faithfulness assumption devising scalable Bayesian methods for exact search. Although our method is constraint-based, we use methods in the other categories as baselines to compare against (Section 5). We briefly provide overviews of them below.

FCM-based CSL methods assume a specific functional form and noise distribution to provably recover graphs with asymptotic consistency guarantees. The assumptions underlying these methods are typically stronger than those underlying constraint-based or score-based approaches, but they are usually testable [Bühlmann et al., 2014]. The causal additive model [Bühlmann et al., 2014] is an example of FCM-based CSL, employing also efficient search; it decouples regularisation for variable selection and carries out order estimation via maximum likelihood. Other examples of FCM-based algorithms with different sets of assumptions are those in [Shimizu et al., 2006; Zhang and Hyvärinen, 2009; Rolland et al., 2022].

Score-based CSL treats the search for DAGs fitting the data as an optimisation problem whereby a score is used to measure the best fit. As in constraint-based methods, the main assumption is faithfulness (defined in Section 3) but the search strategy does not involve independence. Greedy equivalent search [Chickering, 2002]

optimises the Bayesian information criterion as a metric to judge the optimal fit of a graph to the data. The procedure is greedy in the sense that it works like a regression, where a variable (or an edge in graph search) is added or removed in a forward and/or backward search to find the best scoring subset. Among others, Ramsey et al. [2017] proposes a scalable version of greedy equivalent search, Huang et al. [2018] a generalised score for greedy equivalent search, and Tsamardinos et al. [2006] use min-max hill-climbing search.

Within the score-based category, another family of methods emerged from the reformulation of acyclicity into a continuous form [Zheng et al., 2018]. This reformulation allows the graph search to be performed with gradients and to employ the machinery used in machine learning optimisation, e.g. stochastic gradient descent. Many works have proposed algorithms based on this paradigm, see Vowels et al. [2022] for an overview. In particular, Zheng et al. [2020] extends [Zheng et al., 2018] to the non-linear setting, while Ng et al. [2022] use gumbel-softmax to derive binary adjacency matrices and reduce the dependence on thresholding of the continuous adjacency matrix output by Zheng et al. [2020]. Other continuous optimisation methods include [Lachapelle et al., 2020; Yu et al., 2019; Khemakhem et al., 2021; Sanchez et al., 2023] among others. These methods are non-parametric and, as opposed to traditional score-based, as well as constraint-based methods, do not assume faithfulness explicitly, since their stochastic nature prevents any formal guarantees.

Other methods exist in the literature, not strictly falling under a single category. These include methods adopting both independence testing and graph/edge scoring e.g. [Claassen and Heskes, 2012; Triantafillou et al., 2014; Ogarrio et al., 2016; Magliacane et al., 2016]. Different approaches are based on Supervised Learning [Dai et al., 2023], Reinforcement Learning [Sauter et al., 2023], Generative Flow Networks [Deleu et al., 2022], Bayesian methods [Rittel and Tschitschek, 2023] and Optimal Transport [Tu et al., 2022]. These methods are mentioned here for completeness but will not play a role in the paper.

3 Preliminaries

We introduce notation and describe the previously proposed modifications of the PC-algorithm, facilitating the understanding of our proposed method.

3.1 Graph Notation

A graph $\mathcal{G} = (\mathbf{V}, E)$, is made up of a set of nodes $\mathbf{V} = \{X_1, \dots, X_d\}$ and a set of edges $E \subseteq \mathbf{V} \times \mathbf{V}$. The nodes correspond to random variables, while the edges reflect the (binary) relationships between variables. A graph can be *directed* if it contains only directed edges (\rightarrow); *undirected* if it only has undirected edges ($-$) and *partially directed* if it has both. The *skeleton* \mathcal{C} of a (partially) directed graph is the result of replacing all directed edges with undirected ones. A graph is *acyclic*

if there is no directed path (collection of directed edges) that begins and ends with the same variable, in which case it is called a directed acyclic graph (DAG). If an edge exists between two variables then the two variables are adjacent. The set of adjacent nodes to a node X_i , according to a graph \mathcal{G} , is denoted by $\text{adj}(\mathcal{G}, X_i)$. A node X_j in $\text{adj}(\mathcal{G}, X_i)$ is called a parent of X_i if $X_j \rightarrow X_i$. The set of parents of X_i is denoted by $\text{pa}(\mathcal{G}, X_i)$. A triple (X_i, X_j, X_k) is called an *Unshielded Triple (UT)* if two variables are not adjacent but each is adjacent to the third, denoted as $X_i - X_j - X_k$.

Each variable takes values from its own domain. Two variables X_i, X_j are *independent*, given a conditioning set $\mathbf{S} \subseteq \mathbf{V} \setminus \{X_i, X_j\}$, if fixing the values of the variables in \mathbf{S} , X_i or X_j does not provide any additional information about X_j or X_i (resp.). In this case, we write $X_i \perp\!\!\!\perp X_j \mid \mathbf{S}$ and call \mathbf{S} a *separating set* for X_i, X_j . A separating set is a set of variables that *d-separates* two other (sets) of variables, by rendering them independent (see Pearl [2009] for a formal definition). A UT can be oriented as a *v-structure* $X_i \rightarrow X_j \leftarrow X_k$, where X_j is called a *collider*, by virtue of d-separation, as a collider is a variable that makes dependent other two variables that are independent otherwise. Hence, if we observe $X_1 \perp\!\!\!\perp X_2$ and $X_1 \not\perp\!\!\!\perp X_2 \mid X_3$ we can infer that X_3 is a collider for X_1 and X_2 , making $X_1 - X_3 - X_2$ a v-structure, i.e. $X_1 \rightarrow X_3 \leftarrow X_2$.

A DAG can be interpreted causally [Spirtes et al., 2000; Pearl, 2009] when arrows are associated to causes and this allows manipulations that represent interventions (experiments) that can uncover the causal effect of a variable upon another, without performing the actual experiments, and only leveraging observational data [Pearl, 2009]. Causal *sufficiency* is the assumption that no latent common causes (confounders) are missing from the data. Probabilistic measures are needed in practice to relate graphs to observational data.

3.2 Statistical Notation

A joint distribution P factorizes according to a DAG \mathcal{G} if $P(\mathbf{V}) = \prod_{i=1}^d P(X_i \mid \text{pa}(\mathcal{G}, X_i))$. P is said Markovian w.r.t. a DAG \mathcal{G} if the conditional independence relations entailed by \mathcal{G} via d-separation are respected in the distribution P . In turn, distribution P is *faithful* w.r.t. \mathcal{G} if the opposite is true, and the conditional independences in P imply the d-separation relations from DAG \mathcal{G} . Different DAGs can imply the same set of conditional independences, in which case they form a Markov Equivalence Class (MEC, [Richardson and Spirtes, 1999]). DAGs in a MEC present the same adjacencies and v-structures and are uniquely represented by a *completed partially DAG* (CPDAG) [Chickering, 2002]. A CPDAG is a partially directed graph that has a directed edge if every DAG in the MEC has it and an undirected edge if both directions appear in different DAGs belonging to the MEC.

A *Conditional Independence Test (CIT)*, e.g. Fisher’s Z [Fisher, 1970], HSIC [Gretton et al., 2007], or KCI [Zhang et al., 2011], is a procedure whereby a test statis-

tic measuring independence is constructed with a known asymptotic distribution under the null hypothesis \mathcal{H}_0 of independence. Calculating the test statistic on a given dataset allows to calculate the p -value (or observed significance level) of the test for that data, under \mathcal{H}_0 . This is a measure of evidence against \mathcal{H}_0 [Hung et al., 1997]. Under \mathcal{H}_0 , p is uniformly distributed in the interval $[0, 1]$ which allows to set a significance level α that represents the pre-experiment Type I error rate (rejecting \mathcal{H}_0 when it is true), whose expected value is at most α . A CIT, denoted by $I(X_i, X_j \mid \mathbf{S})$, outputs an observed significance level p . If $I(X_i, X_j \mid \mathbf{S}) = p \geq \alpha$ then $I_\alpha = \top$ and $X_i \perp\!\!\!\perp X_j \mid \mathbf{S}$. Instead, if $I(X_i, X_j \mid \mathbf{S}) = p < \alpha$ then we can reject \mathcal{H}_0 and declare the variables dependent: $I_\alpha = \perp$ and $X_i \not\perp\!\!\!\perp X_j \mid \mathbf{S}$. Under the alternative hypothesis of dependence \mathcal{H}_1 , the distribution of p depends on the sample size and the true value of the test statistic [Hung et al., 1997]. However, under any condition, the distribution of the p -value is monotonically decreasing and markedly skewed towards 0. This allows for comparing p -values, with the highest p -values bearing the lowest likelihood of dependence [Hung et al., 1997; Ramsey, 2016].

3.3 Shapley Values

The Shapley value $\phi_v(i)$, originally proposed in game theory [Shapley, 1953], represents a player i ’s marginal value-added upon joining a team, averaged over all orderings in which the team can be constructed and weighted by the probability of occurrence. Suppose a team $N = 1, \dots, n$ of players cooperates to earn value $v(N)$. Here v is a value function associating a real number $v(S)$ with any coalition $S \subseteq N$. Then, formally:

$$\phi_v(i) = \sum_{S \subseteq N \setminus \{i\}} \frac{|S|!(n - |S| - 1)!}{n!} [v(S \cup \{i\}) - v(S)] \quad (1)$$

where the first term in the sum is the weighting factor w_S^n and the second is the marginal value according to the value function v . In our method (see Section 4), the value $v(N)$ of the team is the p -value of the biggest conditioning set. The players are the variables, and the possible teams are the various conditioning sets considered when evaluating the independencies to determine the orientation of an UT.

3.4 The PC-algorithm(s)

The PC-algorithm [Spirtes et al., 2000] operates under the assumptions of acyclicity, sufficiency, and faithfulness. It consists of three steps: 1) building a skeleton of the graph via adjacency search; 2) analyzing UTs in the skeleton and orienting these as v-structures, and 3) orienting as many of the remaining undirected edges without creating new v-structures or cycles [Meek, 1995]. The algorithm is computationally efficient, especially for sparse graphs, and has been shown to be sound, complete, [Spirtes et al., 2000] and consistent in the sample limit [Kalisch and Bühlman, 2007; Harris and Drton,

2013]. However, the sample version of the algorithm depends on the order in which the variables are considered.

To address this, PC-stable was proposed [Colombo and Maathuis, 2014], which does not depend on the variables' ordering. For the second step, Majority-PC (MPC) [Colombo and Maathuis, 2014] and Conservative-PC (CPC) [Ramsey et al., 2006] were proposed, which have different decision rules for orienting v-structures. MPC accepts as v-structures only the UTs that have the potential collider appearing in less than half of the separating sets of the other two nodes, while CPC orients a v-structure if the collider under consideration is found in none of the separating sets.

Max-PC [Ramsey, 2016] proposes another decision rule for orienting v-structures involving the use of p -values. The decision rule selects the conditional independence test with the maximum p -value and only orients the v-structure if the conditioning set for this test does not contain the collider under consideration.

Finally, ML4C treats the v-structure orientation as a supervised learning problem: it trains a machine learning model on synthetic examples of v-structures and then predicts a binary label to decide upon UTs at test time.

In summary, several decision rules have been proposed to improve a critical step of the PC-algorithm. CPC is conservative, MPC proposes a middle-ground rule, Max-PC is informed by the observed significance level of the tests, and ML4C introduces a black-box model that adds model uncertainty to the estimation. All these methods aim to improve on Step 2 of the PC-algorithm by providing a decision rule on the identification of v-structures.

4 Shapley-PC

We aim at improving the discovery of v-structures, and hence the overall accuracy of the graph extracted from the data, by lowering the dependence on a single wrong test when deciding about colliders with sample data.

We propose to choose the v-structures based on the Shapley value of the variable under consideration to be a collider when evaluating an UT, by defining a principled decision rule based on game theory, where we analyse the behaviour of the observed significance level when adding a candidate collider to the conditioning set, regardless of what is already in it. Shapley values are very well suited for the task in that they calculate the marginal value-added of a player (a variable) upon joining a team (a conditioning set).

For \mathcal{C} a given skeleton, $X_i - X_j - X_k$ an UT in \mathcal{C} and

$$\mathbf{N} = \{\mathbf{S} | \mathbf{S} \subseteq \text{adj}(\mathcal{C}, X_i) \setminus \{X_j\} \vee \mathbf{S} \subseteq \text{adj}(\mathcal{C}, X_k) \setminus \{X_j\}\} \quad (2)$$

the adjacency sets of X_i, X_k to evaluate, we define *Shapley Independence Value (SIV)* as follows:

$$\begin{aligned} \phi_I(X_j, \{X_i, X_k\}) &= \\ &= \sum_{\mathbf{S} \in \mathbf{N}} w_{\mathbf{S}}^n [I(X_i, X_k | \mathbf{S} \cup \{X_j\}) - I(X_i, X_k | \mathbf{S})] \quad (3) \end{aligned}$$

where $w_{\mathbf{S}}^n$ is the same weighting as in Eq. 1 where n is the number of variables X in \mathbf{N} . Applying Eq. 3, we

Algorithm 1 Shapley-PC

Input: $I_\alpha(X_i, X_j | \mathbf{S}) \forall X_i, X_j \in \mathbf{V}, \mathbf{S} \subseteq \mathbf{V} \setminus \{X_i, X_j\}$

Step 1: Adjacency Search [Colombo and Maathuis]

```

1:  $\mathcal{C} \leftarrow$  complete graph over  $\mathbf{V}$ 
2: for  $X_i \in \mathcal{C}$  do
3:   for  $X_k \in \text{adj}(\mathcal{C}, X_i)$  do
4:     for  $\mathbf{S} \in \mathbf{N}$  do
5:       Remove edge from  $\mathcal{C}$  iff  $X_i \perp\!\!\!\perp X_k | \mathbf{S}$ 
   return  $\mathcal{C}$ 

```

Step 2: Orient v-structures

```

6:  $SV \leftarrow \emptyset$ 
7: for  $X_i - X_j - X_k \in \mathcal{C}$  do
8:   for  $\mathbf{S} \in \mathbf{N}$  do ▷From Eq. 2
9:     for  $X_c \in \mathbf{S}$  do
10:       $SV \leftarrow SV \cup \{\phi_I(X_c, \{X_i, X_k\})\}$ 
11:      $\phi_I^* = \min(SV)$  ▷Least contribution to  $I()$ 
12:     if  $\phi_I^* = \phi_I(X_j, \{X_i, X_k\})$  then
13:       if  $X_i - X_j - X_k$  not fully directed then
14:         if do not add a cycle then
15:           orient:  $X_i \rightarrow X_j \leftarrow X_k$ 
   return PDAG

```

Step 3: Apply Rules for Patterns [Meek, 1995] to PDAG

Return: CPDAG

recover the marginal contribution $\phi_I(X_j, \{X_i, X_k\})$ of a candidate collider X_j to the observed significance level of the independence test between the other two variables X_i, X_k of the UT, when it enters the conditioning set \mathbf{S} , regardless of the order in which it enters. Following [Ramsey, 2016; Hung et al., 1997], the higher the p -value, the higher the likelihood of independence. The lower $\phi_I(X_j, \{X_i, X_k\})$, the lower is the contribution of variable X_j to the independence of the common parents X_i, X_k , hence the maximum likelihood of it being a collider. This is our decision rule: we declare colliders the variables with the lowest ϕ_I among the nodes adjacent to X_i, X_k .

SIVs have some useful properties that help maintaining the soundness of the original PC-algorithm given perfect conditional independence information. In order to prove soundness, we encode the concept of perfect conditional information into a *perfect CIT*: a test that is able to extract perfect conditional independence information from data.

Definition 1. A perfect CIT I is defined as:

$$I(X_i, X_j | \mathbf{S}) = \begin{cases} 1 & \text{iff } X_i \perp\!\!\!\perp X_j | \mathbf{S} \\ 0 & \text{otherwise} \end{cases}$$

Using Definition 1, we show the consistent behaviour of SIVs for the evaluation of colliders within UT.

Theorem 1. Given a skeleton \mathcal{C} and an UT $X_i - X_j - X_k \in \mathcal{C}$, with a perfect CIT I , $\phi_I(X_j, \{X_i, X_k\}) < 0$ if X_j is a collider and $\phi_I(X_j, \{X_i, X_k\}) > 0$ otherwise.

Proof. A perfect CIT, as per Definition 1, will result in $I(X_i, X_k | \mathbf{S} \cup \{X_j\}) = 0$ if X_j is a collider for X_i, X_k

and 1 otherwise. Since for any UT $X_i - X_j - X_k$, X_j is either in all or none of the separating sets for X_i, X_k [Spirtes et al., 2000, Lemma 5.1.3], then $[I(X_i, X_k | \mathbf{S} \cup \{X_j\}) - I(X_i, X_k | \mathbf{S})] = -1 \forall \mathbf{S} \subseteq \mathbf{V} \setminus \{X_i, X_j\}$ if it is a collider, and 1 otherwise. Finally, the weighting in Eq. 3 will not change the sign of ϕ_I , only its magnitude, hence the sign of ϕ_I will identify colliders. \square

Theorem 1 states that given correct conditional independence information, a decision rule to identify colliders based on SIV is correct. This allows us to prove the soundness of our modified PC-algorithm.

Theorem 2. *Let P be faithful to a DAG $\mathcal{G} = (\mathbf{V}, E)$, and assume that we are given perfect conditional independence information about all pairs of variables $(X_i, X_j) \in \mathbf{V}$ given subsets $\mathbf{S} \subseteq \mathbf{V} \setminus \{X_i, X_j\}$. Then the output of the SPC-algorithm is the CPDAG that represents \mathcal{G} .*

Proof. The skeleton of the CPDAG is correct as proven in [Colombo and Maathuis, 2014, Theorem 2]. Given that $\phi_I(X_j, \{X_i, X_k\}) < 0 \forall X_j$ that are colliders by Theorem 1, the decisions about the v-structures will be correct. Lastly, the propagation rules in Step 3 of Alg. 1 are applied and their soundness and completeness have been proved by Meek [1995]. Hence the CPDAG output by Shapley-PC represents the true \mathcal{G} . \square

A sketch of our proposed method Shapley-PC is provided in Alg. 1. The first step is the adjacency search that outputs a skeleton \mathcal{C} that input our decision rule in Step 2. Note that the Step 1 we report is a simplified version of the original PC-Stable Colombo and Maathuis [2014], in particular the increasing size of the conditioning set is omitted for conciseness. For Step 2, we calculate SIVs for all the variables adjacent to X_i and X_k when testing if X_j is a collider in the UT under consideration: $X_i - X_j - X_k \in \mathcal{C}$ (lines 6-10). Note that the amount of tests performed here is the same as in CPC, MPC and Max-PC, but we extract more granular information and analyse it using SIVs. Our decision rule (lines 11-15) is to declare X_j a collider if it has the lowest contribution to the observed significance level. Two further conditions are applied: as in PC-Max, we avoid bi-directed edges by checking orientation before adding the edges; additionally we check for acyclicity before making the orientation. If we would add a bi-directed edge or a cycle, then the v-structure is not oriented.

Note that in this paper we adopt a rather conservative approach and choose only the most negative ϕ_I to be defined as a collider. This is a heuristic in line with the idea of maximising p -values [Ramsey, 2016]. However, different rules can be crafted depending on the problem analysed. For example one could choose all the variables with negative ϕ_I or that have $\phi_I < \tau$ with τ set at some threshold, e.g. the median, mean, or highest change.

By analysing all possible combinations of conditioning sets we have less dependence on a wrong test and render SPC order-independent as CPC and MPC. Furthermore, we remove the dependency on the significance threshold α for Step 2 of the PC-algorithm. We note that $\phi_I(X_j, \{X_i, X_k\})$ is calculated for the adjacency sets of

X_i, X_k , hence a wrong edge removal in Step 1 of Alg. 1 would imply that we do not consider that variable in our conditioning sets. This trait is shared across all PC-based methods.

In the sample limit, the original PC-algorithm has been shown to be consistent for sparse graphs and multivariate Gaussian distributions [Kalisch and Bühlman, 2007] or Gaussian copulas [Harris and Drton, 2013]. The results are contingent on PC only performing CIT between pairs of variables, with the size of the conditioning sets \mathbf{S} less or equal to the degree of the graph. Our proposed method shares these characteristic with its predecessors, hence the consistency results are equally applicable.

As in PC, the complexity of our algorithm depends on the number of vertices and their maximal degree [Spirtes et al., 2000, p.85]. As in CPC, MPC and PC-Max, we perform additional tests compared to the original PC, that used the separating sets derived from the adjacency search in Step 1. The number of tests though still depends on the graph degree, as we only add the tests about the adjacency sets of X_i, X_k to calculate $\phi_I(X_j, \{X_i, X_k\})$. As noted by Ramsey et al. [2006], the majority of the testing is still done in the adjacency search of Step 1 of Alg. 1.

Next, we empirically demonstrate the usefulness of Shapley-PC in extracting causal graphs from finite samples.

5 Experiments

We run experiments on both synthetic (Section 5.1) and real data (Section 5.2). We compare Shapley-PC (SPC) against baselines from constraint-based, score-based and FCM-based methods. We include Max-PC from the former category since it is the best performing compared to CPC or MPC. From the continuous score-based search methods, we consider Notears-MLP [Zheng et al., 2020] and MCSL-MLP [Ng et al., 2022], since they are the best performing according to reported results.¹ From the greedy score-based literature, we also compare against FGS [Ramsey et al., 2017] and from the FCM-based algorithms we use CAM [Bühlmann et al., 2014]. The last two were chosen as they proved competitive in the experiments by [Zheng et al., 2018, 2020; Ng et al., 2022; Lachapelle et al., 2020]. Finally, we include a Random baseline as in [Lachapelle et al., 2020], by just sampling 10 random graphs to compare to the true graphs for each run. Details on the baselines and the implementation, including code to reproduce the experiments, are in Section A.1 and A.2 in the Appendix.

Evaluation Metrics. We report normalised Structural Hamming Distance (SHD) for both the experiments on synthetic and real data. SHD counts the number of changes (adding or removing an edge

¹We did not include GraN-DAG [Lachapelle et al., 2020] since its performance in our experiments was always lower than NOTEARS or MCSL.

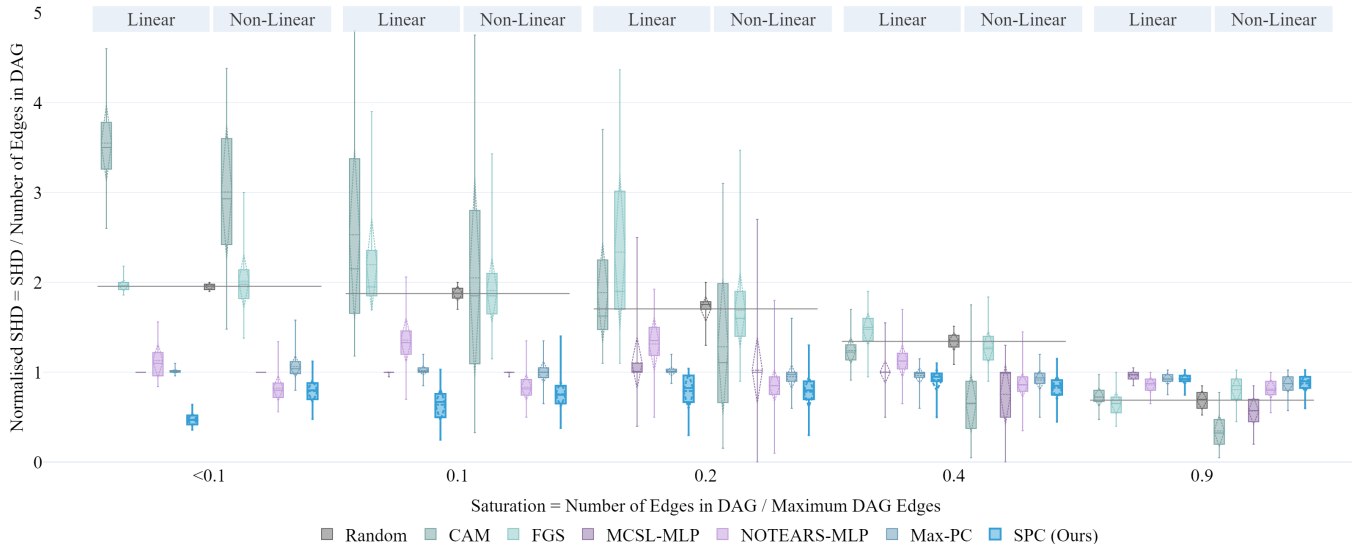


Figure 1: Experiments with synthetic data. We report Normalised Structural Hamming Distance (y-axis) against our proposed saturation parameter ζ on the x-axis for linear and non-linear SEMs. See text for details.

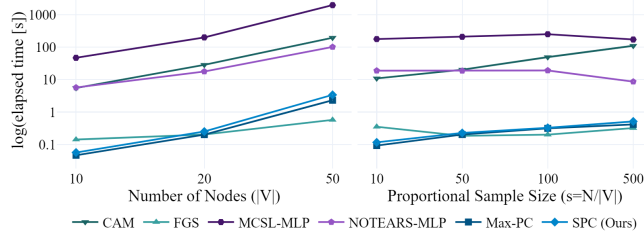


Figure 2: Runtime comparison. We report the elapsed time in seconds (log scale) against number of nodes (left plot) and proportional sample size (right plot).

or changing an orientation) needed to recover the true graph from the estimated one. Normalised SHD is SHD divided by the number of edges in the ground truth graph to be recovered. We use normalised SHD to be able to aggregate over the different graph sizes. All metrics are calculated on the true underlying DAG rather than on the associated CPDAG. Since GES, Max-PC and SPC (Ours) output a CPDAG and not a full DAG, we gave undirected edges a penalty, treating them as missing edges.

To show the differences in performance among the different methods, we define a metric called *saturation* (ζ) of the graph, defined as the proportion of edges in a DAG over the maximum number allowed in a DAG of that size to remain acyclic. In particular, the maximum number of edges $E^M = |\mathbf{V}| \times (|\mathbf{V}| - 1)/2$. As an example, saturation for a graph with $|\mathbf{V}| = 10$ and $d = 4$ is $\zeta = |\mathbf{V}| \times d/E^M = 0.9$, while for $|\mathbf{V}| = 50$ and $d = 4$, $\zeta = 0.16$. Note that $d = |E|/|\mathbf{V}|$ is usually referred as the density (or sparsity) parameter. Although the number of edges change with $|\mathbf{V}|$ for a fixed d , this is not really capturing the sparsity of the graph. This can be

noted from the additional plots presented in Section A.4 in the Appendix. Additional details about the metrics used are reported in Section A.3 of the Appendix where we report also additional metrics, including SID [Peters and Bühlmann, 2015], precision and recall (Sections A.4 and A.5, for synthetic and real data, respectively).

5.1 Synthetic Data

Data Generating Processes (DGPs). We analyse all the different DGPs in [Zheng et al., 2018, 2020] for Erdős-Rényi (ER) graphs. In each experiment, 10 random graphs $\mathcal{G}_i = (\mathbf{V}, E)$ were generated from the ER model. Graphs change across two dimensions: $|\mathbf{V}| \in \{10, 20, 50\}$ and density $d = \{1, 2, 4\}$ with $|E| = |\mathbf{V}| \times d$.

Given the ground truth DAG \mathcal{G}_i , we simulate 8 different additive noise Structural Equation Models (SEMs) of the type $X_j = f_j(\text{pa}(\mathcal{G}, X_j)) + u_j$ for all $j \in [1, \dots, |\mathbf{V}|]$ in topological order, 4 linear and 4 non-linear. For the linear SEMs f_j is linear with coefficients \mathbf{W} initialised uniformly randomly. We then sample $\mathbf{X} = \mathbf{W}^T \mathbf{X} + u$ where the noise u is generated from Gaussian, Exponential, Gumbel and Uniform distributions. For the non-linear models the noise model u remains Gaussian but four different f_j are adopted: Gaussian processes (GPs), additive models with GPs, mixed index models and multi-layer perceptrons. We vary the number of drawn samples (N) in function of the number of nodes $N = s \times |\mathbf{V}|$, $s \in \{10, 50, 100, 500\}$.

Unlike previous works [Zheng et al., 2018, 2020; Lachapelle et al., 2020; Ng et al., 2022], we provide a comparison on standardised data. This approach reduces the target leak problem described by Reisach et al. [2021]. The additive nature of the DGP creates a clue for algorithms to follow when deciding parents-children relations, as children will always have higher variance compared to their parents and grandparents in the causal

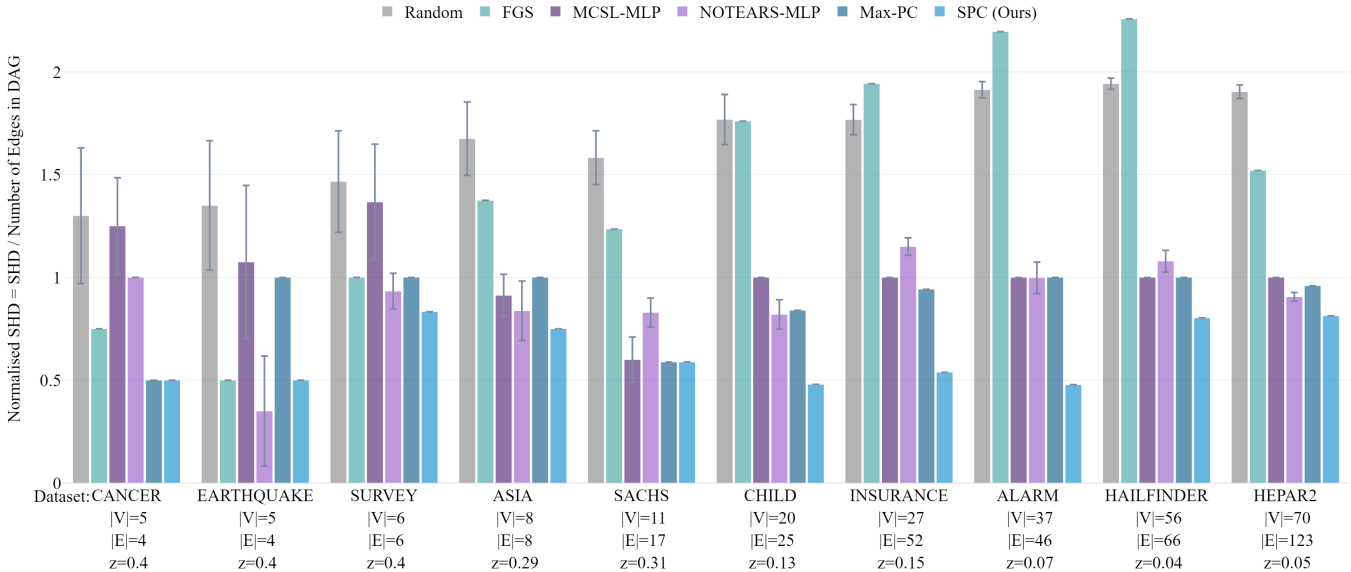


Figure 3: Experiments with real data from the `bnlearn` repository. We report Normalised Structural Hamming Distance (y-axis, the lower the better) for 8 dataset. For each dataset we report number of nodes ($|V|$), number of edges ($|E|$) and saturation parameter (z , referred to as ζ in the text).

chain. This effect is measured by a metric named varsortability [Reisach et al., 2021]. After standardisation, the varsortability of our synthetic data resulted to be zero in all scenarios, indicating no target leak. More details on the DGPs are provided in Section A.4 in the Appendix.

Results. Our results for the different DGPs described are visualised in Fig. 1. We report normalised SHD by our proposed graph saturation metric ζ , and aggregate the different SEMs into the broader classes of linear and non-linear. Results by SEM are provided in Section A.4 in the Appendix, together with additional metrics such as SID [Peters and Bühlmann, 2015], precision and recall. Further evaluation metrics such as false/true positive, negative and discovery rates are provided in our repository² together with interactive versions of the plots that allow the inspections of the values behind them.

From Fig. 1 we can see that SPC is competitive across almost all scenarios. At a high level, SPC works best for sparse graphs with linear SEMs but it remains competitive for non-linear SEMs.

It is well known that PC-algorithms perform best on sparse graphs [Kalisch and Bühlman, 2007] and it is clearly visible in Fig. 1 through our saturation metric. Although SPC’s performance worsens for higher saturation, the change is not as marked as for other methods. We note that we always perform better than Max-PC, the method most similar to our proposed one, demonstrating the effectiveness of our SIV decision rule. Interestingly, among all methods compared, CAM and FGS are the most affected by graph saturation, but in the opposite direction: their performance is worse than random

for sparse graphs but improves significantly for dense ones. The difference is significant for non-linear graphs with $\zeta = 0.9$, where CAM has the best performance of all methods. On the other hand, for $\zeta < 0.2$ CAM performs worst and significantly worse than the random baseline. To be noted that CAM is specifically built for additive noise models, which should be an advantage. As for the MLP-based methods, NOTEARS is on par with SPC for most of non-linear scenarios but significantly worse in all linear ones. MCSL is better than NOTEARS and SPC only for the most saturated DAGs with non-linear DGPs. We attribute the worse performance of SPC in non-linear scenarios to the independence test we used: Fisher’s Z. This could be swapped for more complex tests that account for non-linearity, e.g. KCI [Zhang et al., 2011].

Judging performance based on SID and recall (reported in Fig. 4 and Fig. 5 in the Appendix) our SPC outperforms all baselines for linear, sparse DAGs ($\zeta \leq 0.1$); matches CAM and surpasses the other baselines for non-sparse linear scenarios and equals NOTEARS, improving on the other baselines except CAM for non-linear cases. In terms of precision (Fig. 6 in the Appendix), our SPC tops for all linear scenarios except $\zeta \geq 0.9$, where FGS is better, and equals NOTEARS, with others underperforming except for non-linear data and $\zeta \geq 0.4$, where MCSL leads.

In Fig. 2 we show a comparison of run times. FGS is the quickest and best-scaling method. SPC and Max-PC follow on par. The MLP-based methods and CAM have much higher run times. Note that although the relative increase in time for SPC and Max-PC is steeper than FGS for increasing number of nodes, this is still a fraction compared to the MLP-based and CAM methods.

²<https://github.com/briziorusso/ShapleyPC>

5.2 Real Data

We perform experiments on ten common benchmark datasets from the `bnlearn` repository [Scutari, 2014] (see Section A.5 in the Appendix for more detail). Results against our baselines³ are reported in Fig. 3. We report number of nodes, edges and the saturation parameter for each dataset and measure normalised SHD, as in our synthetic experiments (SID, precision and recall are provided in the Appendix, Section A.5). From Fig. 3 we can see that SPC performs the best on seven out of the ten datasets. We note that we are never statistically significantly worse than any baselines and that the baselines performance follows the one observed in the synthetic experiments: the most saturated graphs are the hardest for Shapley-PC to correctly predict. However, the overall performance is the most consistent across the datasets and shows the value-added of our proposed method for real applications.

6 Conclusion

We proposed a decision rule for orienting v-structures within constraint-based CSL algorithms. The method is based on Shapley values, an established concept from game theory [Shapley, 1953]. We implement our decision rule within the PC-stable algorithm by Colombo and Maathuis [2014], proposing Shapley-PC and prove that our decision rule does not invalidate the soundness and consistency guarantees of the base algorithm.

We carried out an extensive evaluation of our method against several baselines, showing that it performs best in most scenarios. We also showed the impact of sparsity of the underlying DAG on the performance of all methods analysed and that the results on real data follow the findings on synthetic data. Additionally, our experiments were carried out on standardised data, which makes the causal ordering more difficult but also more general and applicable to real scenarios.

Interesting lines of future work include applying our approach to methods that do not assume causal sufficiency or acyclicity (e.g. FCI [Spirtes et al., 2000; Mooij and Claassen, 2020], CCD [Richardson and Spirtes, 1999]) or to score-based methods like FSG [Ramsey et al., 2017]. It would also be interesting to change the decision rule into more/less conservative versions and to analyse the informativeness of our proposed SIV to an interactive discovery process involving humans.

³Note that CAM returned errors related to the rank of the adjacency matrix when processing this data, hence excluded.

Acknowledgments. This research was partially funded by UKRI [grant number EP/S023356/1], in the CDT in Safe and Trusted AI, by J.P. Morgan and by the Royal Academy of Engineering under the Research Chairs and Senior Research Fellowships scheme and by the European Research Council (ERC) under the European Union’s Horizon 2020 research and innovation programme (grant agreement No. 101020934, ADIX). The authors would like to thank Ruben Menke, Antonio Rago, Avinash Kori and Torgunn Ringsø for their helpful feedback in the build up to this work. Any views or opinions expressed herein are solely those of the authors.

References

- Bühlmann, P., Peters, J., and Ernest, J. (2014). CAM: Causal additive models, high-dimensional order search and penalized regression. *The Annals of Statistics*, 42(6):2526–2556.
- Chickering, D. M. (2002). Learning equivalence classes of bayesian-network structures. *J. Mach. Learn. Res.*, 2:445–498.
- Claassen, T. and Heskes, T. (2012). A bayesian approach to constraint based causal inference. In *Proceedings of the Twenty-Eighth Conference on Uncertainty in Artificial Intelligence, UAI’12*, page 207–216, Arlington, Virginia, USA. AUAI Press.
- Colombo, D. and Maathuis, M. H. (2014). Order-independent constraint-based causal structure learning. *J. Mach. Learn. Res.*, 15(1):3741–3782.
- Colombo, D., Maathuis, M. H., Kalisch, M., and Richardson, T. S. (2012). Learning high-dimensional directed acyclic graphs with latent and selection variables. *The Annals of Statistics*, 40(1):294–321.
- Dai, H., Ding, R., Jiang, Y., Han, S., and Zhang, D. (2023). MI4c: Seeing causality through latent vicinity. In *Proceedings of the 2023 SIAM International Conference on Data Mining (SDM)*, pages 226–234. SIAM.
- Deleu, T., Góis, A., Emezue, C., Rankawat, M., Lacoste-Julien, S., Bauer, S., and Bengio, Y. (2022). Bayesian structure learning with generative flow networks. In *Uncertainty in Artificial Intelligence*, pages 518–528. PMLR.
- Fisher, R. A. (1970). Statistical methods for research workers. In *Breakthroughs in statistics: Methodology and distribution*, pages 66–70. Springer.
- Frye, C., Rowat, C., and Feige, I. (2020). Asymmetric shapley values: incorporating causal knowledge into model-agnostic explainability. In *Advances in Neural Information Processing Systems*, volume 33, pages 1229–1239. Curran Associates, Inc.
- Glymour, C., Zhang, K., and Spirtes, P. (2019). Review of causal discovery methods based on graphical models. *Frontiers in genetics*, 10:524.

- Gretton, A., Fukumizu, K., Teo, C., Song, L., Schölkopf, B., and Smola, A. (2007). A kernel statistical test of independence. In *Advances in Neural Information Processing Systems*, volume 20. Curran Associates, Inc.
- Harris, N. and Drton, M. (2013). Pc algorithm for non-paranormal graphical models. *Journal of Machine Learning Research*, 14(69):3365–3383.
- Heskes, T., Sijben, E., Bucur, I. G., and Claassen, T. (2020). Causal shapley values: Exploiting causal knowledge to explain individual predictions of complex models. In *Advances in Neural Information Processing Systems*, volume 33, pages 4778–4789. Curran Associates, Inc.
- Huang, B., Zhang, K., Lin, Y., Schölkopf, B., and Glymour, C. (2018). Generalized score functions for causal discovery. In *Proceedings of the 24th ACM SIGKDD International Conference on Knowledge Discovery & Data Mining, KDD 2018, London, UK, August 19-23, 2018*, pages 1551–1560. ACM.
- Hung, H. M. J., O’Neill, R. T., Bauer, P., and Kohne, K. (1997). The behavior of the p-value when the alternative hypothesis is true. *Biometrics*, 53(1):11–22.
- Ichiishi, T. (1983). *Game Theory for Economic Analysis*. Economic Theory, Econometrics, and Mathematical Economics. Elsevier Science.
- Kalisch, M. and Bühlman, P. (2007). Estimating high-dimensional directed acyclic graphs with the pc-algorithm. *Journal of Machine Learning Research*, 8(22):613–636.
- Khemakhem, I., Monti, R., Leech, R., and Hyvarinen, A. (2021). Causal autoregressive flows. In *International conference on artificial intelligence and statistics*, pages 3520–3528. PMLR.
- Lachapelle, S., Brouillard, P., Deleu, T., and Lacoste-Julien, S. (2020). Gradient-based neural dag learning. In *International Conference on Learning Representations*.
- Lundberg, S. M. and Lee, S.-I. (2017). A unified approach to interpreting model predictions. In *Proceedings of the 31st International Conference on Neural Information Processing Systems, NIPS’17*, page 4768–4777, Red Hook, NY, USA. Curran Associates Inc.
- Magliacane, S., Claassen, T., and Mooij, J. M. (2016). Ancestral causal inference. *Advances in Neural Information Processing Systems*, 29.
- Meek, C. (1995). Causal inference and causal explanation with background knowledge. In *Proceedings of the Eleventh Conference on Uncertainty in Artificial Intelligence, UAI’95*, page 403–410, San Francisco, CA, USA. Morgan Kaufmann Publishers Inc.
- Mooij, M. J. and Claassen, T. (2020). Constraint-based causal discovery using partial ancestral graphs in the presence of cycles. In *Proceedings of the 36th Conference on Uncertainty in Artificial Intelligence (UAI)*, volume 124 of *Proceedings of Machine Learning Research*, pages 1159–1168. PMLR.
- Ng, I., Zheng, Y., Zhang, J., and Zhang, K. (2021). Reliable causal discovery with improved exact search and weaker assumptions. In Ranzato, M., Beygelzimer, A., Dauphin, Y., Liang, P., and Vaughan, J. W., editors, *Advances in Neural Information Processing Systems*, volume 34, pages 20308–20320. Curran Associates, Inc.
- Ng, I., Zhu, S., Fang, Z., Li, H., Chen, Z., and Wang, J. (2022). Masked gradient-based causal structure learning. In *Proceedings of the 2022 SIAM International Conference on Data Mining (SDM)*, pages 424–432. SIAM.
- Ogarrio, J. M., Spirtes, P., and Ramsey, J. (2016). A hybrid causal search algorithm for latent variable models. In Antonucci, A., Corani, G., and Campos, C. P., editors, *Proceedings of the Eighth International Conference on Probabilistic Graphical Models*, volume 52 of *Proceedings of Machine Learning Research*, pages 368–379, Lugano, Switzerland. PMLR.
- Pearl, J. (2009). *Causality*. Cambridge University Press, 2 edition.
- Peters, J. and Bühlmann, P. (2015). Structural intervention distance for evaluating causal graphs. *Neural computation*, 27(3):771–799.
- Peters, J., Janzing, D., and Schölkopf, B. (2017). *Elements of causal inference: foundations and learning algorithms*. The MIT Press.
- Ramsey, J. (2016). Improving accuracy and scalability of the pc algorithm by maximizing p-value.
- Ramsey, J., Glymour, M., Sanchez-Romero, R., and Glymour, C. (2017). A million variables and more: the fast greedy equivalence search algorithm for learning high-dimensional graphical causal models, with an application to functional magnetic resonance images. *International journal of data science and analytics*, 3:121–129.
- Ramsey, J., Spirtes, P., and Zhang, J. (2006). Adjacency-faithfulness and conservative causal inference. In *Proceedings of the Twenty-Second Conference on Uncertainty in Artificial Intelligence, UAI’06*, page 401–408, Arlington, Virginia, USA. AUAI Press.
- Reisach, A. G., Seiler, C., and Weichwald, S. (2021). Beware of the simulated dag! causal discovery benchmarks may be easy to game. In *Advances in Neural Information Processing Systems 34: Annual Conference on Neural Information Processing Systems 2021, NeurIPS 2021, December 6-14, 2021, virtual*, pages 27772–27784.
- Richardson, T. and Spirtes, P. (1999). Automated Discovery of Linear Feedback Models. In *Computation, Causation, and Discovery*. AAAI Press.

- Rittel, S. and Tschiatschek, S. (2023). Specifying prior beliefs over dags in deep bayesian causal structure learning. In *ECAI 2023 - 26th European Conference on Artificial Intelligence, September 30 - October 4, 2023, Kraków, Poland - Including 12th Conference on Prestigious Applications of Intelligent Systems (PAIS 2023)*, volume 372 of *Frontiers in Artificial Intelligence and Applications*, pages 1962–1969. IOS Press.
- Rolland, P., Cevher, V., Kleindessner, M., Russell, C., Janzing, D., Schölkopf, B., and Locatello, F. (2022). Score matching enables causal discovery of nonlinear additive noise models. In *International Conference on Machine Learning*, pages 18741–18753. PMLR.
- Sanchez, P., Liu, X., O’Neil, A. Q., and Tsaftaris, S. A. (2023). Diffusion models for causal discovery via topological ordering. In *The Eleventh International Conference on Learning Representations*.
- Sauter, A. W., Acar, E., and François-Lavet, V. (2023). A meta-reinforcement learning algorithm for causal discovery. In *Conference on Causal Learning and Reasoning*, pages 602–619. PMLR.
- Schölkopf, B., Locatello, F., Bauer, S., Ke, N. R., Kalchbrenner, N., Goyal, A., and Bengio, Y. (2021). Toward causal representation learning. *Proceedings of the IEEE*, 109(5):612–634.
- Scutari, M. (2014). Bayesian network repository. <http://www.bnlearn.com/bnrepository>.
- Shapley, L. S. (1953). A value for n-person games (1953). *Contribution to the Theory of Games*.
- Shimizu, S., Hoyer, P. O., Hyvärinen, A., and Kerminen, A. (2006). A linear non-gaussian acyclic model for causal discovery. *J. Mach. Learn. Res.*, 7:2003–2030.
- Spirtes, P., Glymour, C. N., and Scheines, R. (2000). *Causation, prediction, and search*. MIT press.
- Triantafillou, S., Tsamardinos, I., and Roupelaki, A. (2014). Learning neighborhoods of high confidence in constraint-based causal discovery. In *Probabilistic Graphical Models: 7th European Workshop, PGM 2014, Utrecht, The Netherlands, September 17-19, 2014. Proceedings 7*, pages 487–502. Springer.
- Tsamardinos, I., Brown, L. E., and Aliferis, C. F. (2006). The max-min hill-climbing bayesian network structure learning algorithm. *Machine learning*, 65:31–78.
- Tu, R., Zhang, K., Kjellstrom, H., and Zhang, C. (2022). Optimal transport for causal discovery. In *International Conference on Learning Representations*.
- Vowels, M. J., Camgoz, N. C., and Bowden, R. (2022). D’ya like dags? a survey on structure learning and causal discovery. *ACM Computing Surveys*, 55(4):1–36.
- Yu, Y., Chen, J., Gao, T., and Yu, M. (2019). DAG-GNN: DAG structure learning with graph neural networks. In Chaudhuri, K. and Salakhutdinov, R., editors, *Proceedings of the 36th International Conference on Machine Learning*, volume 97 of *Proceedings of Machine Learning Research*, pages 7154–7163. PMLR.
- Zanga, A., Ozkirimli, E., and Stella, F. (2022). A survey on causal discovery: Theory and practice. *International Journal of Approximate Reasoning*, 151:101–129.
- Zhang, K. and Hyvärinen, A. (2009). On the identifiability of the post-nonlinear causal model. In *Proceedings of the Twenty-Fifth Conference on Uncertainty in Artificial Intelligence, UAI ’09*, page 647–655, Arlington, Virginia, USA. AUAI Press.
- Zhang, K., Peters, J., Janzing, D., and Schölkopf, B. (2011). Kernel-based conditional independence test and application in causal discovery. In *Proceedings of the Twenty-Seventh Conference on Uncertainty in Artificial Intelligence, UAI ’11*, page 804–813, Arlington, Virginia, USA. AUAI Press.
- Zheng, X., Aragam, B., Ravikumar, P., and Xing, E. P. (2018). Dags with NO TEARS: continuous optimization for structure learning. In *Advances in Neural Information Processing Systems 31: Annual Conference on Neural Information Processing Systems 2018, NeurIPS 2018, December 3-8, 2018, Montréal, Canada*, pages 9492–9503.
- Zheng, X., Dan, C., Aragam, B., Ravikumar, P., and Xing, E. (2020). Learning sparse nonparametric dags. In *Proceedings of the Twenty Third International Conference on Artificial Intelligence and Statistics*, volume 108 of *Proceedings of Machine Learning Research*, pages 3414–3425. PMLR.

Appendix

A Details on Experiments

In this section we provide additional details for the experiments in Section 5 of the main text.

A.1 Baselines

We used the following five baselines with respective implementations (see Section 2 and 3 for context):

- PC-Max⁴ [Ramsey, 2016] is a modification of the PC-algorithm [Spirtes et al., 2000] where, similarly to our proposed algorithm SPC, the author proposes an improved decision rule to select v-structures. For comparison to our proposed algorithm (Alg. 1 in the main text), a sketch of the PC-Max decision rule is provided in Alg. 2.
- Fast Greedy equivalence Search (FGS)⁵ [Ramsey et al., 2017] is a fast implementation of GES [Chickering, 2002] where graphs are evaluated using the Bayesian Information Criterion (BIC) upon addition or deletion of given edge, in a greedy fashion, involving the evaluation of insertion and removal of edges in a forward and backward fashion.
- Causal Additive Model (CAM)⁶ [Bühlmann et al., 2014] learns an additive Structural Equation Model (SEM) by decoupling feature selection (carried out through penalised regression) and causal order estimation via efficient search.
- NOTEARS-MLP⁷ [Zheng et al., 2020] learns a non-linear SEM via continuous optimisation. Having a Multi-Layer Perceptron (MLP) at its core, this method should adapt to different functional dependencies among the variables. The optimisation is carried out via augmented Lagrangian with a continuous formulation of the acyclicity constraint [Zheng et al., 2018].
- Masked-CSL-MLP⁸ [Ng et al., 2022] learns a non-linear SEM via continuous optimisation in the same fashion as Zheng et al. [2020] but applying the gumbel-softmax trick to transform the continuous adjacency matrices into binary and use them as masks. Also this method is MLP-based, hence flexible in regard to functional forms of the SEMs to be modelled.

A.2 Implementation

We provide an implementation of Shapley-PC based on the `causal-learn` python package.⁹ Within

⁴<https://github.com/py-why/causal-learn>

⁵<https://github.com/bd2kccd/py-causal>

⁶<https://github.com/cran/CAM> but called by <https://github.com/FenTechSolutions/CausalDiscoveryToolbox>

⁷<https://github.com/xunzheng/notears>

⁸<https://github.com/huawei-noah/trustworthyAI>

⁹<https://github.com/py-why/causal-learn>

Algorithm 2 Orient V-Structures: Max-PC

Input: Skeleton \mathcal{C}

```
1:  $candUT \leftarrow \emptyset$ 
2: for  $X_i - X_j - X_k \in \mathcal{C}$  do
3:    $pv \leftarrow \emptyset$ 
4:   for  $\mathbf{S} \subseteq \text{adj}(\mathcal{C}, X_i) \cup \text{adj}(\mathcal{C}, X_k)$  do
5:      $p_r \leftarrow I(X_i, X_k | \mathbf{S}_r)$ 
6:      $pv \leftarrow pv \cup (\mathbf{S}_r, p_r)$ 
7:      $(\mathbf{S}^*, p^*) = \text{max}_p(pv)$ 
8:     if  $X_j \notin \mathbf{S}^*$  then
9:        $candUT \cup (X_i - X_j - X_k, p^*)$ 
10: sort( $candUT$ ) by  $p^*$ 
11: for  $X_i - X_j - X_k \in candUT$  do
12:   if  $X_i - X_j - X_k$  not fully directed then
13:     orient:  $X \rightarrow X_j \leftarrow X_k$ 
```

Return: PDAG

`causal-learn`, we define a new PC function that accommodates our decision rule. The code is available at the following repository: <https://github.com/briziorusso/ShapleyPC>. In the repository, we also made available the code to reproduce all experiments and we saved all the plots, presented herein and in the main text, in HTML format. Downloading and opening them in a browser allows the inspection of all the numbers behind the plots in an interactive way.

Hyperparameters. We used default parameters for all the methods. For PC-Max and SPC (ours) we used Fisher Z test [Fisher, 1970], as implemented in `causal-learn`, with significance threshold $\alpha = 0.01$.

Computing infrastructure. Our proposed method, together with Max-PC, FGS and CAM do not benefit from GPU acceleration. All the results were ran on Intel(R) Xeon(R) w5-2455X CPU with 4600 max MHz and 128GB of RAM. The MLP based methods (NOTEARS and MCSL) were ran on NVIDIA(R) GeForce RTX 4090 GPU with 24GB dedicated RAM.

A.3 Evaluation Metrics

As in [Zheng et al., 2018, 2020; Lachapelle et al., 2020], we evaluated the estimated graphs with seven commonly used metrics:

- Structural Hamming Distance (SHD) = E + M + R
- Structural Intervention Distance (SID)
- Precision = TP/(TP + FP)
- Recall = TP/(TP + FN)
- False Discovery Rate (FDR) = (R + FP)/P
- True Positive Rate (TPR) = TP/T
- False Positive Rate (FPR) = (R + FP)/F

where True (T) is the set of true edges while False (F) is the set of non-edges. Positive (P) is the set of estimated edges; Extra (E) is the set of extra edges and Missing

(M) are the ones missing from the skeleton of the true graph. True Positive (TP) is the number of estimated edges with correct direction; Reversed (R) have incorrect direction; False Positive (FP) is an edge which is not in the skeleton of the true graph. True Negative (TN) and False Negative (FN) are edges that are not in the true graph and correctly (resp, incorrectly) removed from the estimated graph. SID was proposed by [Peters and Bühlmann, 2015] and quantifies the agreement to a causal graph in terms of interventional distributions. It aims at quantifying the incorrect causal inference estimations stemming out of a mistake in the causal graph estimation, akin to a downstream task error on a pre-processing step.

From the graphs in Section A.4, we noted how the performance of most of the algorithms tested depended on the sparsity of the graph, which is not very well captured by the common *density* parameter $d = E/|\mathbf{V}|$. We proposed a reformulation of a DAG sparsity that we call DAG saturation ζ , and depends on the maximum number of edges that the graph \mathcal{G} can have to remain a DAG.

In particular, we define the sparsity of a DAG $\mathcal{G} = (\mathbf{V}, E)$ as:

$$\zeta = \frac{2 \times |\mathbf{V}| \times d}{|\mathbf{V}| \times (|\mathbf{V}| - 1)} \quad (4)$$

where $|\mathbf{V}|$ is the number of nodes in \mathcal{G} , d is the density parameter that determines the number of edges $E = |\mathbf{V}| \times d$ and, at the denominator, is the double of the maximum number of edges in \mathcal{G} for it to remain acyclic.

Furthermore, to be able to compare across sparsity, with graphs of different number of nodes and edges, we use normalised SHD, calculated as the ratio of SHD and the number of edges in the true graph.

A.4 Synthetic Data

Here we present details on the experiments with synthetic data from Section 5.1 of the main text.

DGP Details

We analyse all the different DGPs in [Zheng et al., 2018, 2020] for Erdős-Rényi (ER) graphs.

In each experiment, 10 random graphs $\mathcal{G}_i = (\mathbf{V}, E)$ were generated from the ER model. Graphs change across two dimensions: number of nodes $|\mathbf{V}| \in \{10, 20, 50\}$ and density $d = \{1, 2, 4\}$ with the number of edges $|E| = |\mathbf{V}| \times d$.

Given the ground truth DAGs \mathcal{G}_i , we simulate Structural Equation Models (SEMs) belonging to the Additive Noise Model, formally:

$$X_j = f_j(\text{pa}(\mathcal{G}, X_j)) + u_j \quad \forall j \in [1, \dots, |\mathbf{V}|] \quad (5)$$

where f_j is an arbitrary function and u_j are samples from a noise distribution. We simulate 8 different SEMs, four linear and four non-linear, by changing the functions f_j and the noise distributions u_j .

For the linear SEMs, f_j is linear with coefficients \mathbf{W} initialised uniformly in the range $[-2, -0.5] \cup [0.5, 2]$.

We then sample $\mathbf{X} = \mathbf{W}^T \mathbf{X} + u$ where the noise u is generated from the following four distributions:

- Gaussian: $u \sim \mathcal{N}(0, 1)$
- Exponential: $u \sim E(1)$
- Gumbel: $u \sim G(0, 1)$
- Uniform: $u \sim U(-1, 1)$

For the non-linear SEMs, the noise model u remains Gaussian, but four different functions f_j are adopted:

- Gaussian Processes (GPs): f_j is drawn from a GP with RBF kernel of length-scale 1.
- Additive GPs: $f_j(\text{pa}(\mathcal{G}, X_j)) = \sum_{k \in \text{pa}(\mathcal{G}, X_j)} f_{jk}(X_k)$, where each f_{jk} is drawn from a GP with RBF kernel of length-scale 1.
- Mixed Index Model (MIM): $f_j(\text{pa}(\mathcal{G}, X_j)) = \sum_{m=1}^3 h_m(\sum_{k \in \text{pa}(\mathcal{G}, X_j)} \theta_{jmk} X_k)$, where $h_1 = \tanh$, $h_2 = \cos$, $h_3 = \sin$, and each θ_{jmk} is drawn uniformly in the range $[-2, -0.5] \cup [0.5, 2]$.
- Multi-Layer Perceptron (MLP): f_j is a randomly initialised MLP with one hidden layer of size 100 and sigmoid activation.

We vary the number of drawn samples (N) in function of the number of nodes $N = s \times |\mathbf{V}|$, $s \in \{10, 50, 100, 500\}$. We refer to s as the proportional sample size. After sampling from the described DGPs we standardise the data using the standard scaler from `sklearn`.¹⁰ We standardise all the datasets following the observations by Reisach et al. [2021] that simulated data in the CSL literature would not be representative of real-world applications, given their properties in terms of variance/scale. These properties are in fact used by some CSL algorithms to recover the causal ordering of the variables, but are not guaranteed to be present “in the wild”. See [Reisach et al., 2021] for more details on the rationale and justification for standardising data when simulating data for CSL. Note that we measured varsortability [Reisach et al., 2021] of our synthetic data and it resulted to be zero in all scenarios.

Additional Results

In this section we report additional metrics to the normalised SHD reported in Fig. 1 in the main text. The additional results corroborate the ones presented previously. All the numbers behind the plots can be inspected in more detail in the provided repository¹¹, where extra plots for TPR, FPR and FDR are also provided.

From all additional metrics analysed, the results are in line with Fig.1 in the main text, with SPC showing consistent performance across scenarios but a worsening for very dense graphs, in particular $\zeta = 0.9$ (see Section A.3, Eq. 4 or Section 5.1 in the main text for more details). Judging performance based on SID and recall (reported in Fig. 4 and Fig. 5) our SPC: outperforms all baselines for linear, sparse DAGs ($\zeta \leq 0.1$); matches CAM and surpasses the other baseline for non-sparse linear scenarios

¹⁰<https://scikit-learn.org/stable/modules/generated/sklearn.preprocessing.StandardScaler.html>

¹¹<https://github.com/briziorusso/ShapleyPC>

and equals NOTEARS, improves on the other baselines except CAM for non-linear cases. In terms of precision (Fig. 6), our SPC tops for all linear scenarios except $\zeta \geq 0.9$, where FGS is better, and equals NOTEARS, with others underperforming except for non-linear data and $\zeta \geq 0.4$, where MCSL leads.

Split by SEM. In Fig. 1 of the main text, we aggregate the various SEMs we experiment on into linear and non-linear. Here we report the most granular split for SHD and SID for both linear (see Fig. 10 and 11) and non-linear SEMs (see Fig. 12 and 13). The scenarios reported in this section are split by the usual density parameter d , for direct comparison with previous results in the literature and the metrics are plotted against proportional sample size (number of samples in the dataset divided by the number of nodes in the underlying true graph, $N/|N|$).

From Fig. 10 we can see that for all linear SEMs with $d \in \{1, 2\}$ SPC outperforms all baselines. For $|\mathbf{V}| = 10, d = 4$ SPC, and most baselines, perform worse than random. For $d = 4, |\mathbf{V}| \in \{20, 50\}$ SPC is again the best performing methodology, on par with other baselines. According to SID (Fig. 11), SPC performance is the best, on par with CAM for some scenarios, for $d = 1$ and $d = 2$. Interestingly, Max-PC is the worse performing method in these scenarios, showing the value-added of our decision rule based on the same independence tests. For $d = 4$, FGS is the best performing method, by a significant margin in some instances. This is interesting when compared to SHD, according to which FSG performed the worse in many of the scenarios. This seems to be associated to a very high size of the estimated graph.

Comparing performance across the proportional sample size s for each of the sub-graphs in Fig. 10 and 11, we can see how the different methods deal with data availability. CAM is the most data-hungry, as shown by the steep downward trends for increasing s , followed by MCSL. All the other methods, including ours, are less data hungry and maintain performance with low sample size. NOTEARS-MLP and MCSL’s performance is generally much worse than the authors’ reported results because of the standardization in the data.

From Fig. 12 we notice that SPC is competitive in most non-linear scenarios, according to SHD. For $d = 2$ and SEMs belonging to MIM and MLP, MCSL performs the best. For GPs and additive GPs instead the best performing is CAM, that outperforms all other methods for $d = 4$. Judging by SID (Fig. 13), CAM is the best method across all scenarios, with MCSL following for small graphs ($|\mathbf{V}| = 10$) and SPC in line with the other baselines but always significantly better than its closest counterpart, Max-PC. Note that for SEMs based on GPs (gp, gp-add), for $|\mathbf{V}| = 50$ we could only run $s \in \{10, 50, 100\}$. The sampling process from `sklearn` used to generate these SEMs needs more than 128GB of RAM to build a datasets with sample size $N = 25000$, which was needed for $|\mathbf{V}| = 50$ and $s = 500$.

A.5 Real Data

Here we report details on the experiments with real data from Section 5.2 of the main text.

bnlearn datasets

For the experiments on real data, we used ten datasets from the `bnlearn` repository¹² which is widely used for research in CSL. The datasets are from the small and medium and large categories with number of nodes varying from 5 to 70. Details on the number of nodes, edges, sparsity and saturation of the DAGs underlying these data are reported in Table 1, together with links to a more detailed description on the `bnlearn` repository.

Dataset Name	$ N $	$ E $	ζ	$ E / N $
CANCER	5	4	0.4	0.8
EARTHQUAKE	5	4	0.4	0.8
SURVEY	6	6	0.4	1
ASIA	8	8	0.29	1
SACHS	11	17	0.31	1.55
ALARM	37	46	0.07	1.24
CHILD	20	25	0.13	1.25
INSURANCE	27	52	0.15	1.93
HAILFINDER	56	66	0.04	1.18
HEPAR2	70	123	0.05	1.76

Table 1: Details of real dataset from `bnlearn`.

Having downloaded all the `.bif` files from the repository, we load the Bayesian network and the associated conditional probability tables and sample 2000 observations. We encoded the labels using the label encoder from `sklearn` and successively applied standard scaling to all datasets before running the algorithms.

Additional Results

In Fig. 3 in the main text, we show the results on the ten dataset detailed in Table 1, according to Structural Hamming Distance (SHD). In this section we report additional metrics, in line with the experiments on synthetic data. In particular, we visualise Structural Intervention Distance (SID, Fig. 8) and Estimated Graph Size (EGS, Fig. 9). Precision and Recall are left out because they show very similar trends, but are provided in our repository as interactive plots.

Judging by normalised SID, SID divided by the number of edges in the true graph, our SPC is the best performing method for four out of the ten datasets by a significant difference (CHILD, INSURANCE, ALARM and HEPAR2). For the 5 smaller datasets (CANCER, EARTHQUAKE, SURVEY, ASIA and SACHS) there is no significant difference between SPC (according to a t-test on the difference of means) and the baselines, even the random one, except from CANCER where both SPC and Max-PC outperform all other methods. For the last dataset, HAILFINDER, SPC is the best method on par with NOTEARS. MCSL shows a lower SID only because it returns an empty graph (see Fig. 9).

¹²<https://www.bnlearn.com/bnrepository/>

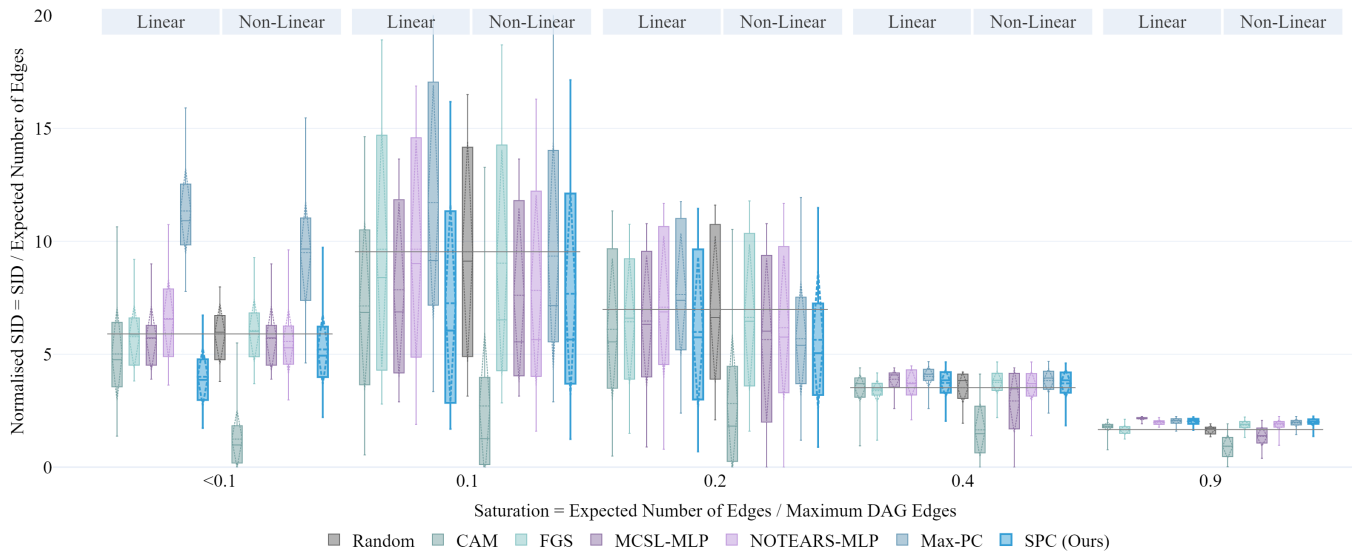


Figure 4: Experiments with synthetic data. We report Normalised Structural Intervention Distance (SID, the lower the better) by saturation (ζ), split by linear and non-linear SEMs.

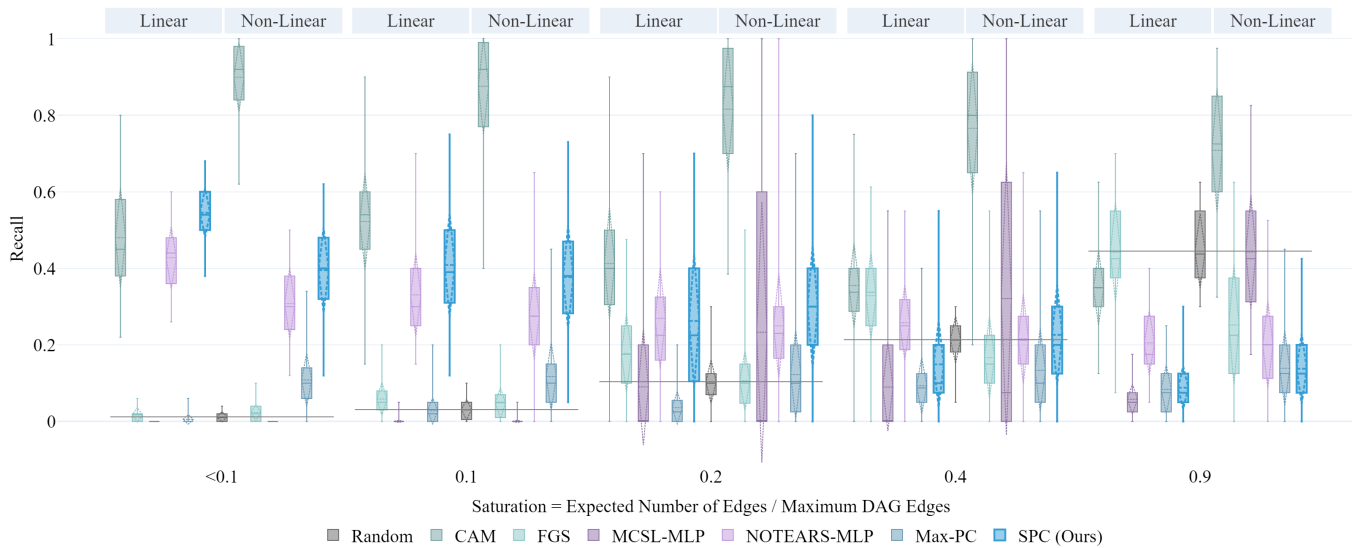


Figure 5: Experiments with synthetic data. We report Recall (the higher the better) by saturation (ζ), split by linear and non-linear SEMs.

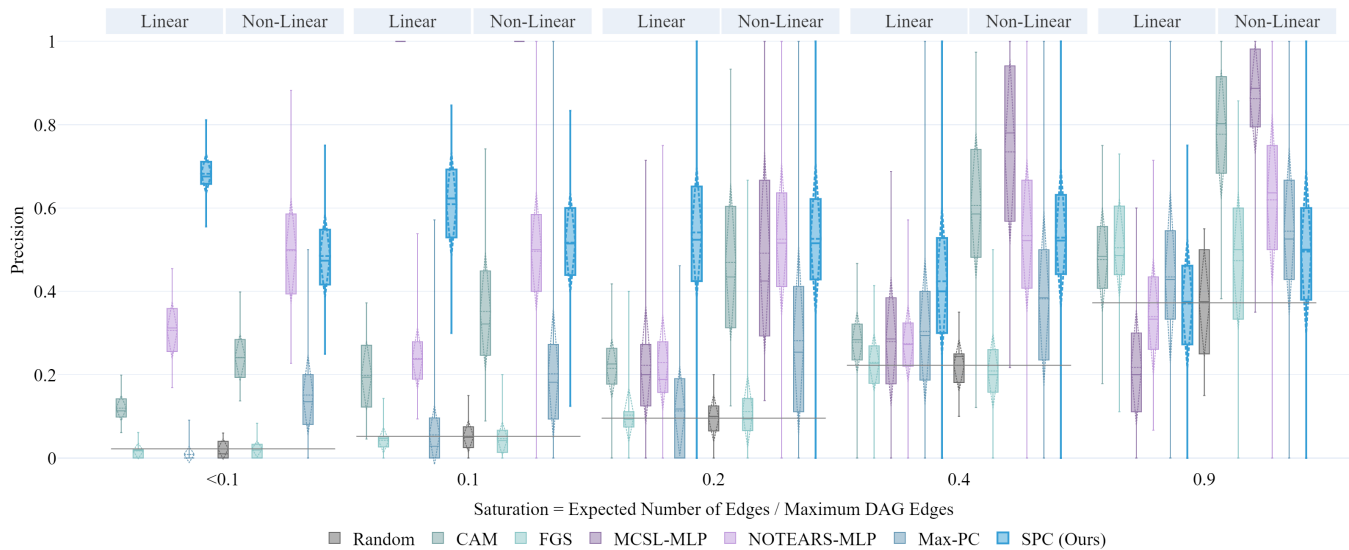


Figure 6: Experiments with synthetic data. We report Precision (the higher the better) by saturation (ζ), split by linear and non-linear SEMs.

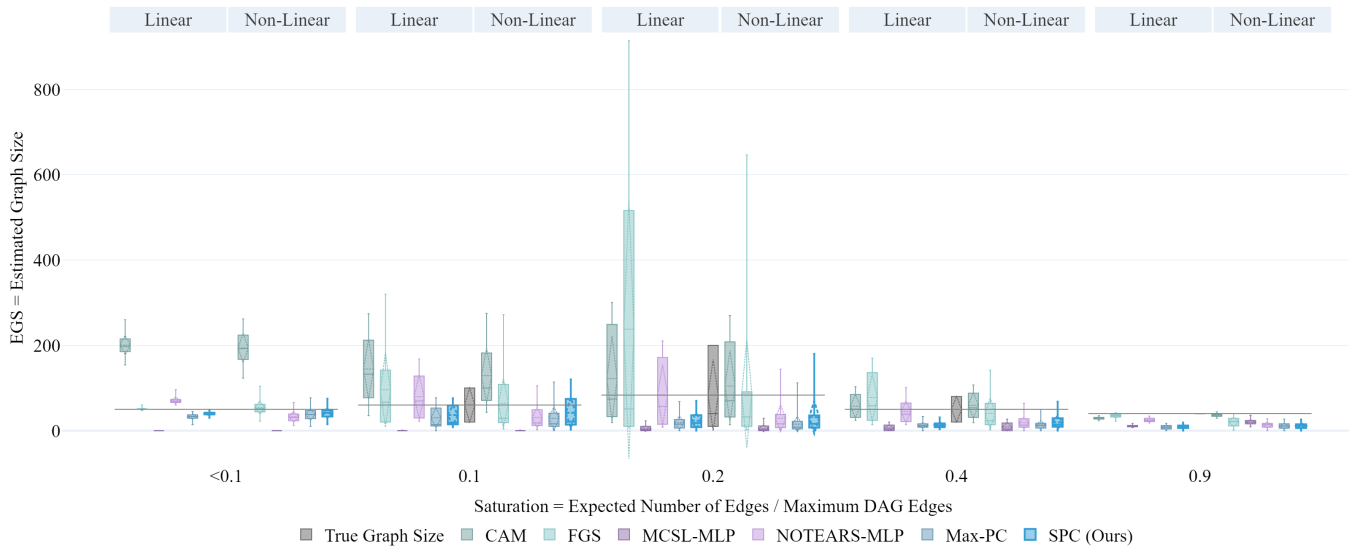


Figure 7: Experiments with synthetic data. We report Estimated Graph Size (EGS) by saturation (ζ), split by linear and non-linear SEMs.

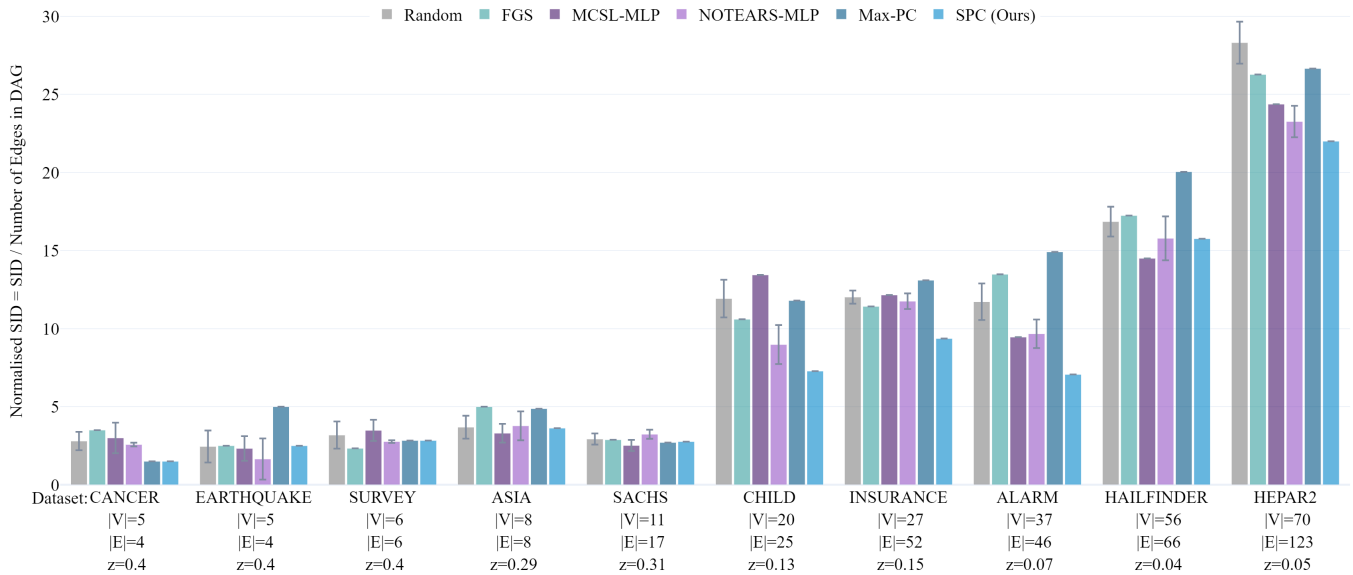


Figure 8: Experiments with real data from the **bnlearn** repository. We report Normalised Structural Intervention Distance (SID, the lower the better) for ten dataset. For each dataset we report number of nodes ($|V|$), number of edges ($|E|$) and saturation (z , referred to as ζ in the text).

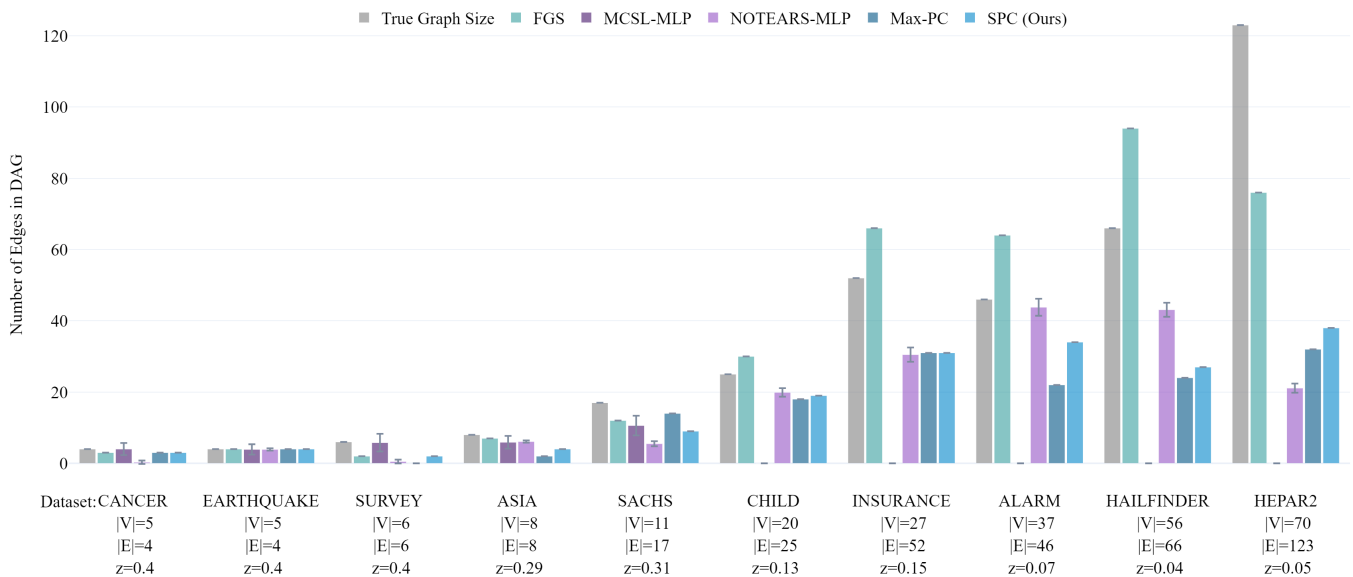


Figure 9: Experiments with real data from the **bnlearn** repository. We report the number of edges in the estimated graph for ten dataset. For each dataset we report number of nodes ($|V|$), number of edges ($|E|$) and saturation (z , referred to as ζ in the text).

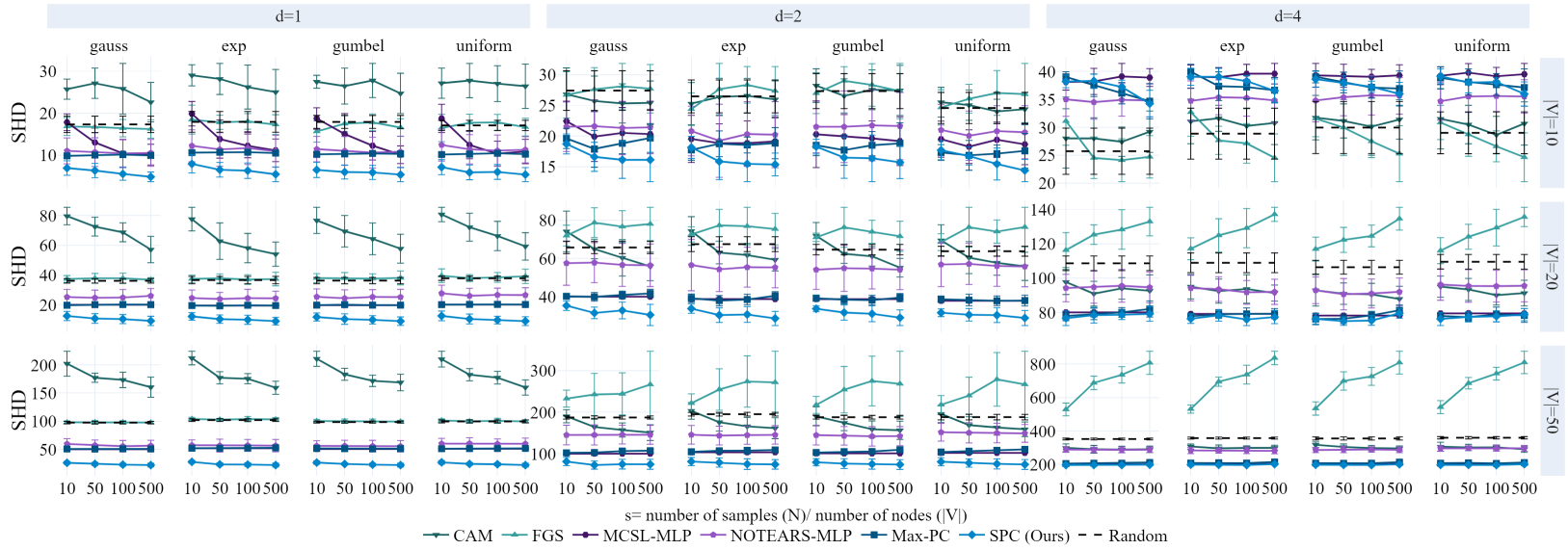


Figure 10: Experiments with synthetic data. We report structural Hamming Distance (SHD, the lower the better) by proportional sample size (s) for number of nodes $|V| \in \{10, 20, 50\}$, expected edges per node $d \in \{1, 2, 4\}$ and linear SEMs with noise sampled from Gaussian (gauss), Gumbel, Exponential (exp) and Uniform distributions (see Section A.1 for more details).

17

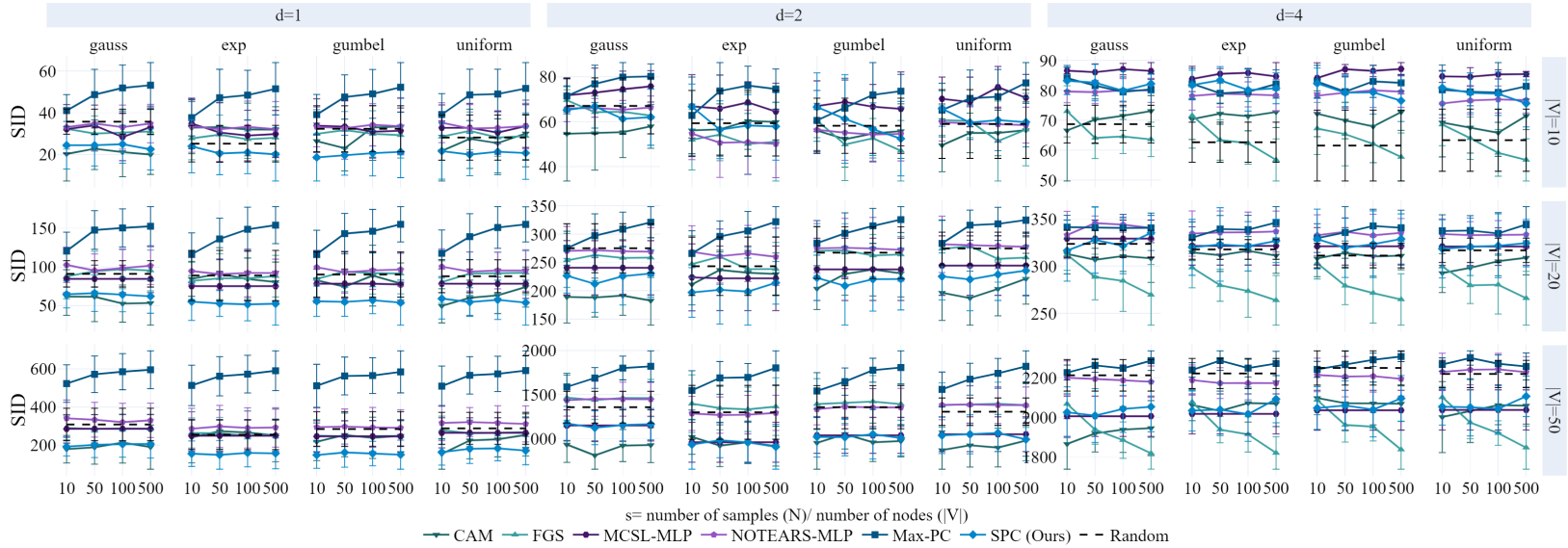


Figure 11: Experiments with synthetic data. We report structural Intervention Distance (SID, the lower the better) by proportional sample size (s) for number of nodes $|V| \in \{10, 20, 50\}$, expected edges per node $d \in \{1, 2, 4\}$ and linear SEMs with noise sampled from Gaussian (gauss), Gumbel, Exponential (exp) and Uniform distributions (see Section A.1 for more details).

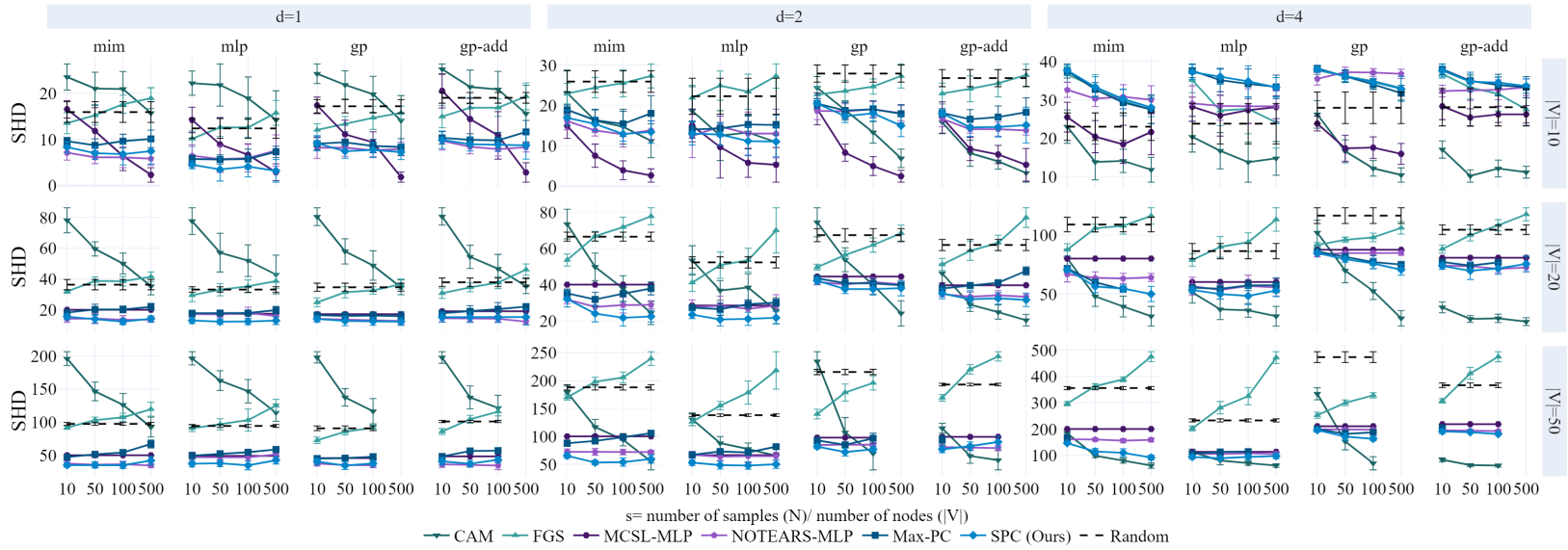


Figure 12: Experiments with synthetic data. We report structural Hamming Distance (SHD, the lower the better) by proportional sample size (s) for number of nodes $|V| \in \{10, 20, 50\}$, expected edges per node $d \in \{1, 2, 4\}$ and non-linear SEMs with functional models f_j sampled from GPs (gp), Additive GPs (gp-add), Mixed Index Models (mim) and MLPs (see Section A.1 for more details).

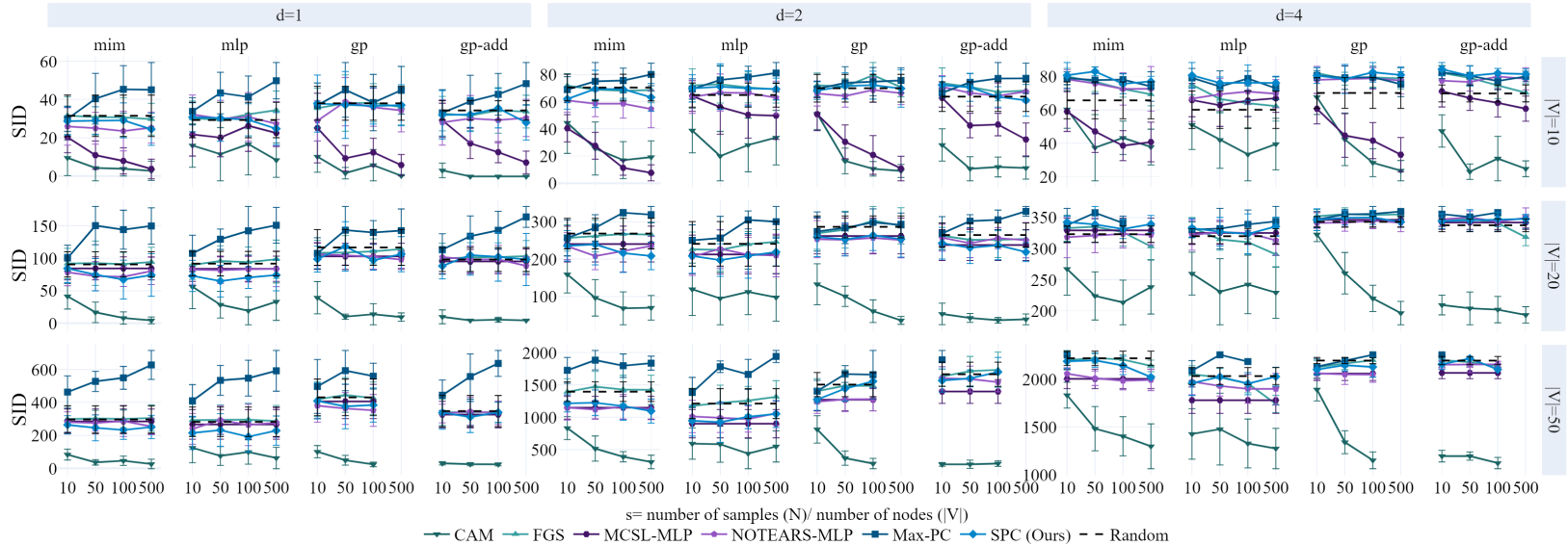


Figure 13: Experiments with synthetic data. We report structural Intervention Distance (SID, the lower the better) by proportional sample size (s) for number of nodes $|V| \in \{10, 20, 50\}$, expected edges per node $d \in \{1, 2, 4\}$ and non-linear SEMs with functional models f_j sampled from GPs (gp), Additive GPs (gp-add), Mixed Index Models (mim) and MLPs (see Section A.1 for more details).